Allosteric Inhibitors

Deutsche Ausgabe: DOI: 10.1002/ange.201511351
Internationale Ausgabe: DOI: 10.1002/anie.201511351

Insights Into the Allosteric Inhibition of the SUMO E2 Enzyme Ubc9

*William M. Hewitt, George T. Lountos, Katherine Zlotkowski, Samuel D. Dahlhauser, Lindsey B. Saunders, Danielle Needle, Joseph E. Tropea, Chendi Zhan, Guanghong Wei, Buyong Ma, Ruth Nussinov, David S. Waugh, and John S. Schneekloth, Jr.**

Abstract: *Conjugation of the small ubiquitin-like modifier (SUMO) to protein substrates is an important disease-associated posttranslational modification, although few inhibitors of this process are known. Herein, we report the discovery of an allosteric small-molecule binding site on Ubc9, the sole SUMO E2 enzyme. An X-ray crystallographic screen was used to identify two distinct small-molecule fragments that bind to Ubc9 at a site distal to its catalytic cysteine. These fragments and related compounds inhibit SUMO conjugation in biochemical assays with potencies of 1.9–5.8 mM. Mechanistic and biophysical analyses, coupled with molecular dynamics simulations, point toward ligand-induced rigidification of Ubc9 as a mechanism of inhibition.*

The posttranslational modification of protein substrates with a small ubiquitin-like modifier (SUMO) tag occurs through a tightly regulated E1/E2/E3 enzymatic cascade and modulates a broad variety of cellular functions.[1] Ubc9 is the only E2 enzyme involved in the conjugation of all three SUMO isoforms to many diverse substrates within the proteome. As a central enzyme in the SUMOylation cycle, Ubc9 is required for normal embryonic development, and it is dysregulated in a variety of disease states such as cancer[2] and ischemia.[3] Ubc9 has been suggested as a potential anticancer target for small-molecule inhibitors, notably for MYC-driven[4] and RAS/Raf-driven[5] cancers, as well as multiple myeloma.[6] Despite its relevance to disease, it has been challenging to identify small molecules that modulate the function of Ubc9. In related ubiquitin-like signaling pathways, inhibitors of E1[7] and E3[8] enzymes are now clinically used as anticancer chemotherapeutics. By contrast, very few reversible inhibitors of any of the approximately 40 known ubiquitin and ubiquitin-like E2 conjugating enzymes have been discovered,[9] only one of which has been characterized in complex with the protein.[10] Thus, new experimentally validated chemical inhibitors of Ubc9 would provide substantial insight into targeting this important enzyme, and potentially E2 enzymes in general.

One powerful approach to identify ligands for challenging protein targets is fragment-based inhibitor discovery.[11] In general, fragment-based approaches leverage sensitive techniques such as NMR, thermal shift, surface plasmon resonance (SPR), or X-ray crystallography to identify low-molecular-weight ligands that bind weakly but specifically to target proteins.[12] Weak leads identified through fragment-based approaches can provide excellent starting points for the development of highly active inhibitors, even in cases where the targets are considered to be challenging, such as protein–protein interactions or so-called "undruggable" targets.[13]

As part of a larger program aimed toward identifying chemical inhibitors of Ubc9, we elected to pursue an X-ray crystallographic fragment screening strategy (see the Supporting Information).[14] Ubc9 crystals diffracting to a resolution of 1.12 Å (PDB ID: 5F6E) were soaked with a series of cocktails, each comprised of three shape-diverse fragments. A total of 352 fragments were screened using this approach, and ligands **1** and **2** (PDB ID: 5F6V and 5F6X, respectively) were identified to bind to Ubc9 (Figure 1). To independently validate the screening results and acquire high-quality data sets, each fragment was then soaked separately into Ubc9 crystals (PDB ID: 5F6W, 5F6Y). Both fragments bound to the same previously unknown allosteric site on Ubc9, which is remote from the catalytic cysteine. The identification of this small-molecule binding site was unanticipated, and to our knowledge has not been predicted.[15] Fragment **1**, 2,2′-biphenol, binds to Ubc9 through a network of hydrogen bonds (Figure 1C). Fragment **2** interacts with Ubc9 at the same site, although primarily through hydrophobic interactions (Figure 1D). In comparison to the *apo* structure of Ubc9, few structural changes were observed upon compound

[*] Dr. W. M. Hewitt, Dr. K. Zlotkowski, S. D. Dahlhauser, Dr. L. B. Saunders, Dr. J. S. Schneekloth, Jr.
Chemical Biology Laboratory, Center for Cancer Research
National Cancer Institute, Frederick, MD 21702 (USA)
E-mail: schneeklothjs@mail.nih.gov

Dr. G. T. Lountos, D. Needle, Dr. J. E. Tropea, Dr. D. S. Waugh
Macromolecular Crystallography Laboratory
Center for Cancer Research
National Cancer Institute, Frederick, MD 21702 (USA)

Dr. G. T. Lountos
Basic Science Program, Leidos Biomedical Research, Inc.
Frederick National Laboratory for Cancer Research
Frederick, MD 21702 (USA)

C. Zhan, Dr. G. Wei
State Key Laboratory of Surface Physics
Key Laboratory for Computational Physical Sciences (MOE)
and Department of Physics
Fudan University, Shanghai (P.R. China)

Dr. B. Ma, Dr. R. Nussinov
Basic Science Program, Leidos Biomedical Research, Inc.
Cancer and Inflammation Program
National Cancer Institute, Frederick, MD 21702 (USA)

Dr. R. Nussinov
Department of Human Genetics and Molecular Medicine
Tel Aviv University, Sackler School of Medicine
Tel Aviv 69978 (Israel)

Supporting information and the ORCID identification number(s) for the author(s) of this article can be found under http://dx.doi.org/10.1002/anie.201511351.

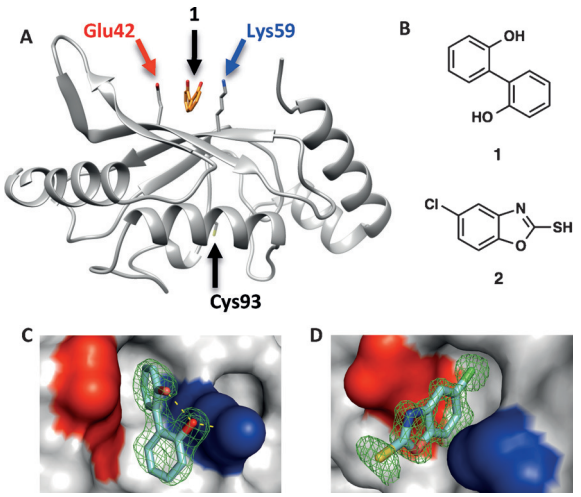

Figure 1. A) Crystal structure of **1** in complex with Ubc9, showing the allosteric binding site relative to the catalytic cysteine (Cys93). B) Structures of fragments **1** and **2**, identified through an X-ray crystallographic screen. Crystal structure of the allosteric binding pocket with bound fragments **1** (C) and **2** (D) are shown overlaid onto the F_o-F_c electron-density map contoured at the 3.0σ level (1.49 and 1.56 Å resolution, respectively), calculated with the fragment omitted from the model. Hydrogen bonds are indicated with yellow dashes.

binding (RMSD = 0.19 Å over 122 Cα atoms, Figure S3 in the Supporting Information).

To validate the binding of each fragment to Ubc9 in solution, a ^{1}H-^{15}N heteronuclear single quantum correlation (HSQC) NMR chemical-shift perturbation experiment was performed.[16] Upon addition of either fragment **1** (Figure 2A) or **3** (a more readily available derivative of **2**, Figure 2B), several statistically relevant chemical-shift perturbations were observed, thus indicating specific binding of both fragments to Ubc9. In both cases, several shifted residues were clustered in or near the binding site identified by X-ray crystallography. In particular, chemical-shift perturbations were observed for Lys59 and Leu60, both of which make direct contact with the two fragments. The binding of both fragments could thus be mapped to the same allosteric binding site observed in crystal structures, thereby confirming that the interactions also occur in solution.

Next, the affinity of each fragment for Ubc9 was measured through SPR (Figure S9). For compound **3**, an equilibrium dissociation constant (K_d) was estimated to be 280 μM. For compound **1**, saturable binding was not achieved, thus indicating a K_d of greater than 2 mM. Both fragments were next tested in a biochemical enzymatic activity assay previously developed in our laboratory[9b] (Figure S1) to evaluate chemical inhibition of SUMOylation by monitoring the conjugation of SUMO-1 to a small peptide substrate at lower enzyme concentrations. Fragments **2** and **3** displayed only weak inhibitory activity up to the limit of solubility. However, fragment **1** completely inhibited SUMOylation with a half-maximal inhibitory concentration (IC_{50}) of 5.8 ± 0.1 mM. Despite its weaker affinity, we considered **1** to be a more desirable starting point for further study owing to its superior activity in the biochemical assay, superior solubility, and a well-defined binding mode that leverages specific hydrogen-bonding interactions between the ligand and Ubc9.

We next synthesized several derivatives of **1** for evaluation (Table 1). HSQC analysis and biochemical evaluation showed that several chemotypes were able to bind to Ubc9 and inhibit SUMOylation. Of particular note are compounds **6** and **8**, which we were able to obtain crystal structures of in complex with Ubc9 at 1.55 Å (PDB ID: 5F6D and 5F6U, respectively), thus showing that these compounds bind at the same allosteric site as **1**. Furthermore, the activity of **8** demonstrates that the core structure of these fragments can be elaborated without diminishing affinity or activity. These fragments are thus suitable for chemical optimization to generate higher-affinity inhibitors.

We next sought to probe the mechanism of action of **1** through a series of thioester bond forming reactions with fluorescently labeled SUMO-1. As expected, **1** had no effect

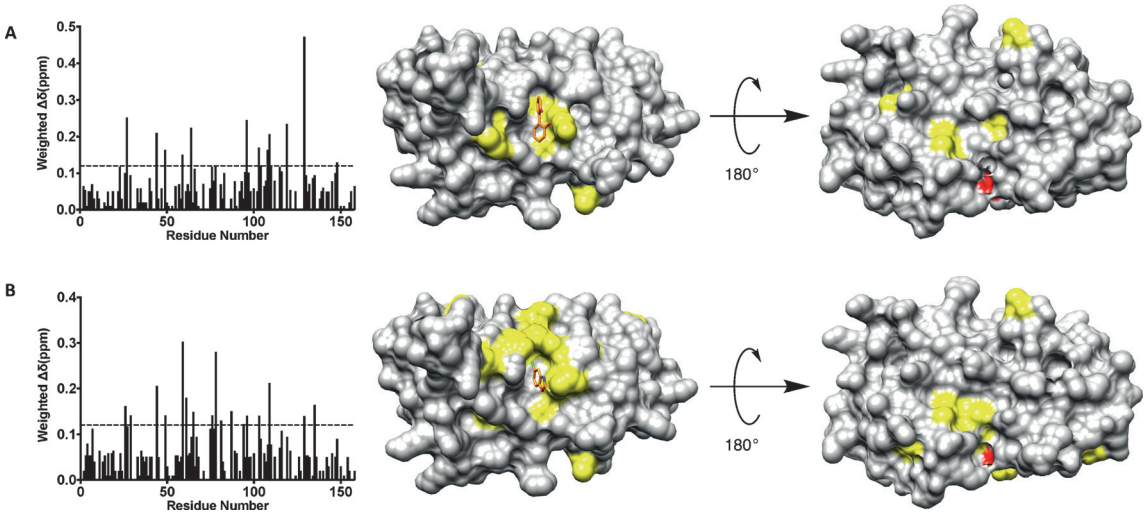

Figure 2. ^{1}H-^{15}N HSQC chemical-shift perturbations of Ubc9 in the presence of **1** (A) and **3** (B). Residues showing statistically relevant perturbations are highlighted in yellow and the catalytic Cys93 is shown in red.

Table 1: Inhibitory concentrations and HSQC data for selected compounds.

Entry	Structure	IC_{50} [mM]	^1H-^{15}N HSQC[a] K59	L60
1		5.8 ± 0.1		
3	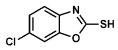	> 3[b]		
4		1.9 ± 0.1		
5		> 20		
6		> 3[b]		
7	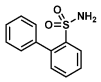	3.1 ± 0.3		
8	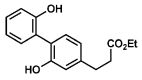	3.0 ± 2.3		

[a] ^1H-^{15}N HSQC with 200 μM Ubc9 in a saturated solution of the compound of interest. Images indicate chemical shifts of selected residues for *apo* (red) and bound (blue) Ubc9. See the Supporting Information for full HSQC spectra. [b] IC_{50} measurement is limited by compound solubility in the assay buffer.

on the formation of the E1–SUMO thioester at relevant concentrations (Figure 3A). However, **1** inhibited formation of the E2–SUMO thioester at concentrations that correlated well with the IC_{50} of the compound (Figure 3B). Furthermore, **1** also inhibited the conjugation of SUMO to the full-length recombinant protein substrate IκBα (Figure 3C) and to a recombinant protein fragment of RanGAP1 (Figure 3D). To demonstrate that the inhibition of SUMOylation was the result of specific binding to this allosteric site, we prepared two Ubc9 binding site mutants. Wild-type Ubc9 (Figure 3E) was compared to both K59A (Figure 3F) and E42A (Figure 3G) mutants. In each case, Ubc9 was able to conjugate SUMO to a fluorescent peptide substrate, thus confirming that the enzymes remain catalytically competent. However, neither mutant was inhibited by **1** at any concentration. Mutation of the binding-site residues thus abolishes inhibitory activity and confirms that specific binding to this site is responsible for inhibition.

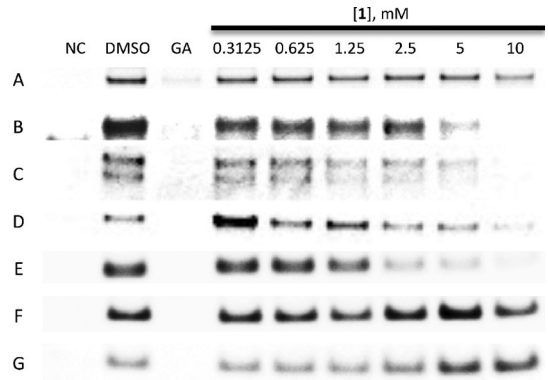

Figure 3. A–D) Effects of **1** on E1–SUMO thioester formation (A), E2—SUMO thioester formation (B), IκBα SUMOylation (C), and RanGAP1 SUMOylation (D) by a fluorescent SUMO protein. E–G) Sumoylation of a fluorescent substrate peptide by wild-type Ubc9 (E), the Ubc9-K59A mutant (F), and the Ubc9-E42A mutant (G). In all cases, negative control (NC) lanes represent assays in the absence of ATP, except for (A) and (B), which were performed in the absence of E1 or E2 enzyme, respectively. GA = ginkgolic acid, 30 μM.

To further investigate the structural basis for the chemical inhibition, we performed molecular dynamics (MD) simulations on Ubc9 in both the presence and absence of either **1** or **8**. Simulations were examined by principal-component analysis (PCA), a technique used to reduce sets of multidimensional variables that describe conformational dynamics into non-degenerate components. The first of these principal components (PC1), which contributes most to the description of overall atomic motions throughout the MD simulations, can be analyzed directly or through the use of covariance matrices, which correlate residue fluctuations.[17]

In both cases, covariance matrices of the *apo* protein revealed a large number of residues with high correlation, thus confirming that Ubc9 is moderately flexible (Figure 4A and Figure S8).[18] In the presence of inhibitor, the majority of these covariance values change considerably, particularly in two loop regions near residues 30 and 133 (Figure 4B, Figure S8B). Additionally, comparison of root mean square fluctuation (RMSF) values for PC1 in the presence of inhibitor demonstrated a substantial decrease in RMSF for almost all residues (Figure 4C and Figure S8C). The largest changes were observed near residues 50–90 (adjacent to the binding site) and 120–140 (near the active-site loops). These experiments, supported by network analysis[19] (Figure S6) and pathway analysis (Figure S7), point toward a model whereby the ligand binding event modulates the dynamics of Ubc9 rather than its conformation, and results in rigidification of the protein in general, with pronounced effects near the active-site loops in addition to the binding site.

In summary, we report the discovery of a previously unknown allosteric small-molecule binding site on the back side of Ubc9 distal from the catalytic site. Our results indicate that compound **1** and related chemotypes bind to Ubc9 and allosterically inhibit SUMOylation through rigidification of Ubc9, ultimately blocking formation of the E2 thioester. Although it remains unclear whether this small-molecule binding pocket plays a role in the overall regulation of SUMOylation in vivo, studies on related E2 enzymes have shown that "backside" protein–protein interactions are involved with the allosteric regulation of their enzymatic activity.[20] In addition, a number of protein–protein interactions occur in close proximity to this site on Ubc9, including noncovalent association with SUMO-1,[21] binding of the SUMO E3 ligase RanBP2,[22] and binding of the SUMO E1 heterodimer, Aos1/Uba2.[23] Compounds that bind to this site could thus perturb a variety of protein–protein interactions that are important for Ubc9 activity, in addition to having

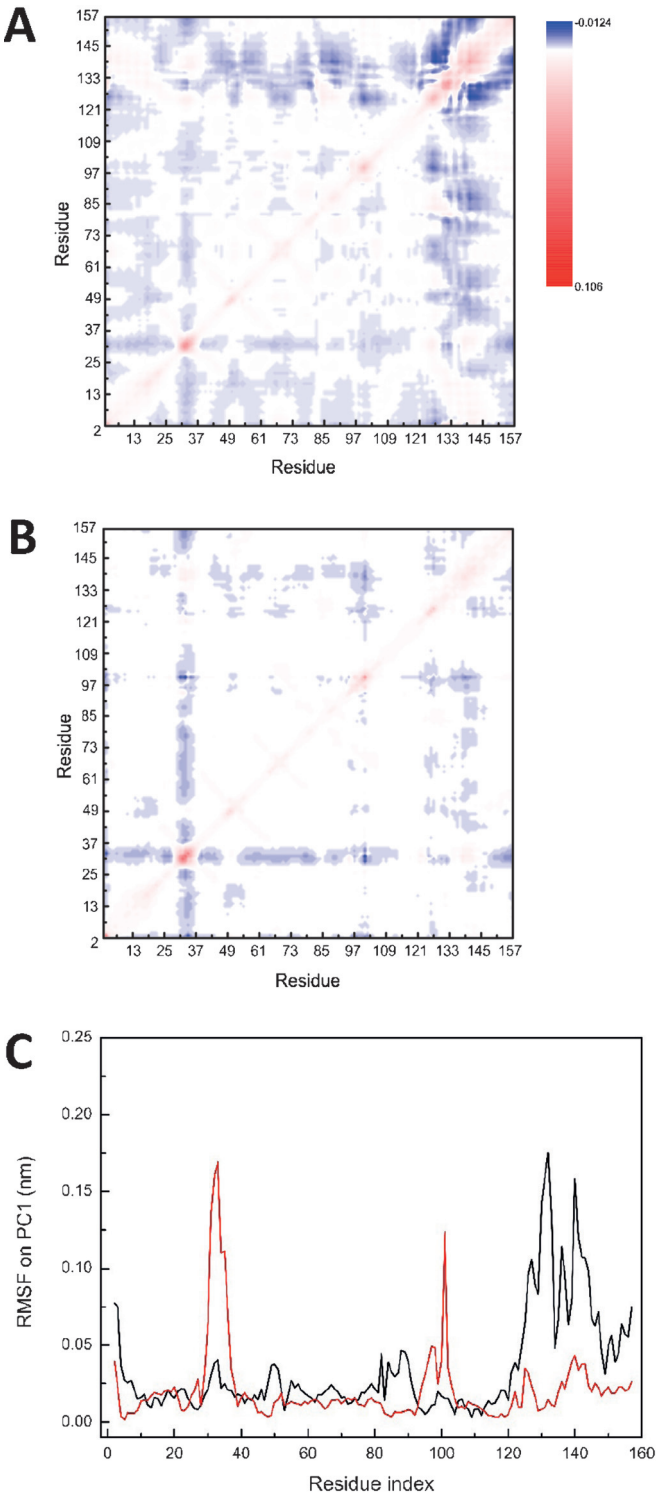

Figure 4. Molecular dynamics simulations of Ubc9. Covariance matrices in the absence (A) and presence (B) of compound **1** are shown. (C) RMSF diagrams projected on PC1 in the absence (black) and presence (red) of **1**.

allosteric effects on Ubc9 itself. Further, this work indicates that allosteric small-molecule binding to Ubc9 may be a viable strategy for the chemical inhibition of SUMOylation and could provide the basis for a general strategy to inhibit E2 enzymes. Work is currently underway to use this information in the design of more potent inhibitors of Ubc9.

Acknowledgements

This project was funded in whole or in part with Federal funds from the Frederick National Laboratory for Cancer Research, National Institutes of Health, under contract HHSN261200800001E and the Intramural Research Program of the NIH, National Cancer Institute, Center for Cancer Research. We thank Dr. T. Andresson and Dr. M. O'Neill (Protein Characterization Lab, CRTP, NCI at Frederick) for help with SPR experiments, and Dr. S. Tarasov and M. Dyba (Biophysics Resource, SBL, NCI at Frederick) for assistance with HRMS studies. X-ray diffraction data were collected at the Southeast Regional Collaborative Access Team (SER-CAT) beamlines 22-ID and 22-BM of the Advanced Photon Source, Argonne National Laboratory. Supporting institutions may be found at http://www.ser-cat.org/members.html. Use of the Advanced Photon Source was supported by the U.S. Department of Energy, Office of Science, Office of Basic Energy Sciences, under contract no. W-31-109-Eng-38.

Keywords: allostery · inhibitors · SUMOylation · Ubc9 · X-ray crystallography

How to cite: *Angew. Chem. Int. Ed.* **2016**, *55*, 5703–5707
Angew. Chem. **2016**, *128*, 5797–5801

[1] a) R. Geiss-Friedlander, F. Melchior, *Nat. Rev. Mol. Cell Biol.* **2007**, *8*, 947–956; b) Z. Hannoun, S. Greenhough, E. Jaffray, R. T. Hay, D. C. Hay, *Toxicology* **2010**, *278*, 288–293.
[2] Y. Y. Mo, Y. N. Yu, E. Theodosiou, P. L. R. Ee, W. T. Beck, *Oncogene* **2005**, *24*, 2677–2683.
[3] Y. J. Lee, Y. Mou, D. Maric, D. Klimanis, S. Auh, J. M. Hallenbeck, *Plos One* **2011**, *6*, e25852.
[4] J. D. Kessler, K. T. Kahle, T. Sun, K. L. Meerbrey, M. R. Schlabach, E. M. Schmitt, S. O. Skinner, Q. Xu, M. Z. Li, Z. C. Hartman, M. Rao, P. Yu, R. Dominguez-Vidana, A. C. Liang, N. L. Solimini, R. J. Bernardi, B. Yu, T. Hsu, I. Golding, J. Luo, C. K. Osborne, C. J. Creighton, S. G. Hilsenbeck, R. Schiff, C. A. Shaw, S. J. Elledge, T. F. Westbrook, *Science* **2012**, *335*, 348–353.
[5] B. Yu, S. Swatkoski, A. Holly, L. C. Lee, V. Giroux, C. S. Lee, D. Hsu, J. L. Smith, G. Yuen, J. Yue, D. K. Ann, R. M. Simpson, C. J. Creighton, W. D. Figg, M. Gucek, J. Luo, *Proc. Natl. Acad. Sci. USA* **2015**, *112*, E1724–1733.
[6] J. J. Driscoll, D. Pelluru, K. Lefkimmiatis, M. Fulciniti, R. H. Prabhala, P. R. Greipp, B. Barlogie, Y. T. Tai, K. C. Anderson, J. D. Shaughnessy, Jr., C. M. Annunziata, N. C. Munshi, *Blood* **2010**, *115*, 2827–2834.
[7] a) J. E. Brownell, M. D. Sintchak, J. M. Gavin, H. Liao, F. J. Bruzzese, N. J. Bump, T. A. Soucy, M. A. Milhollen, X. Yang, A. L. Burkhardt, J. Ma, H. K. Loke, T. Lingaraj, D. Wu, K. B. Hamman, J. J. Spelman, C. A. Cullis, S. P. Langston, S. Vyskocil, T. B. Sells, W. D. Mallender, I. Visiers, P. Li, C. F. Claiborne, M. Rolfe, J. B. Bolen, L. R. Dick, *Mol. Cell* **2010**, *37*, 102–111; b) T. A. Soucy, P. G. Smith, M. A. Milhollen, A. J. Berger, J. M. Gavin, S. Adhikari, J. E. Brownell, K. E. Burke, D. P. Cardin, S. Critchley, C. A. Cullis, A. Doucette, J. J. Garnsey, J. L. Gaulin, R. E. Gershman, A. R. Lublinsky, A. McDonald, H. Mizutani, U. Narayanan, E. J. Olhava, S. Peluso, M. Rezaei, M. D. Sintchak, T. Talreja, M. P. Thomas, T. Traore, S. Vyskocil, G. S.

Weatherhead, J. Yu, J. Zhang, L. R. Dick, C. F. Claiborne, M. Rolfe, J. B. Bolen, S. P. Langston, *Nature* **2009**, *458*, 732 – 736.
[8] a) P. P. Chamberlain, A. Lopez-Girona, K. Miller, G. Carmel, B. Pagarigan, B. Chie-Leon, E. Rychak, L. G. Corral, Y. J. Ren, M. Wang, M. Riley, S. L. Delker, T. Ito, H. Ando, T. Mori, Y. Hirano, H. Handa, T. Hakoshima, T. O. Daniel, B. E. Cathers, *Nat. Struct. Mol. Biol.* **2014**, *21*, 803 – 809; b) A. Lopez-Girona, D. Mendy, T. Ito, K. Miller, A. K. Gandhi, J. Kang, S. Karasawa, G. Carmel, P. Jackson, M. Abbasian, A. Mahmoudi, B. Cathers, E. Rychak, S. Gaidarova, R. Chen, P. H. Schafer, H. Handa, T. O. Daniel, J. F. Evans, R. Chopra, *Leukemia* **2012**, *26*, 2326 – 2335.
[9] a) J. Zmudzki, M. Kamyczek, R. Kwaczynski, *Med Weter* **2002**, *58*, 285 – 287; b) Y. S. Kim, K. Nagy, S. Keyser, J. S. Schneekloth, *Chem. Biol.* **2013**, *20*, 604 – 613; c) C. D. Hodge, R. A. Edwards, C. J. Markin, D. McDonald, M. Pulvino, M. S. Huen, J. Zhao, L. Spyracopoulos, M. J. Hendzel, J. N. Glover, *ACS Chem. Biol.* **2015**, *10*, 1718 – 1728; d) M. A. Sanders, G. Brahemi, P. Nangia-Makker, V. Balan, M. Morelli, H. Kothayer, A. D. Westwell, M. P. Shekhar, *Mol. Cancer Ther.* **2013**, *12*, 373 – 383.
[10] a) D. F. Ceccarelli, X. Tang, B. Pelletier, S. Orlicky, W. Xie, V. Plantevin, D. Neculai, Y. C. Chou, A. Ogunjimi, A. Al-Hakim, X. Varelas, J. Koszela, G. A. Wasney, M. Vedadi, S. Dhe-Paganon, S. Cox, S. Xu, A. Lopez-Girona, F. Mercurio, J. Wrana, D. Durocher, S. Meloche, D. R. Webb, M. Tyers, F. Sicheri, *Cell* **2011**, *145*, 1075 – 1087; b) H. Huang, D. F. Ceccarelli, S. Orlicky, D. J. St-Cyr, A. Ziemba, P. Garg, S. Plamondon, M. Auer, S. Sidhu, A. Marinier, G. Kleiger, M. Tyers, F. Sicheri, *Nat. Chem. Biol.* **2014**, *10*, 156 – 163.
[11] D. E. Scott, A. G. Coyne, S. A. Hudson, C. Abell, *Biochemistry* **2012**, *51*, 4990 – 5003.
[12] D. A. Erlanson, *Top. Curr. Chem.* **2012**, *317*, 1 – 32.
[13] a) M. J. Harner, B. A. Chauder, J. Phan, S. W. Fesik, *J. Med. Chem.* **2014**, *57*, 9687 – 9692; b) H. Jhoti, G. Williams, D. C. Rees, C. W. Murray, *Nat. Rev. Drug Discovery* **2013**, *12*, 644 – 645; c) M. Baker, *Nat. Rev. Drug Discovery* **2013**, *12*, 5 – 7.
[14] J. Badger, *Methods Mol. Biol.* **2012**, *841*, 161 – 177.
[15] X. Duan, J. O. Trent, H. Ye, *Anti-Cancer Agents Med. Chem.* **2009**, *9*, 51 – 54.
[16] Q. Liu, B. Shen, D. J. Chen, Y. Chen, *J. Biomol. NMR* **1999**, *13*, 89 – 90.
[17] G. G. Maisuradze, A. Liwo, H. A. Scheraga, *J. Mol. Biol.* **2009**, *385*, 312 – 329.
[18] Q. Liu, C. Jin, X. Liao, Z. Shen, D. J. Chen, Y. Chen, *J. Biol. Chem.* **1999**, *274*, 16979 – 16987.
[19] Z. Hu, D. Bowen, W. M. Southerland, A. del Sol, Y. Pan, R. Nussinov, B. Ma, *PLoS Comput. Biol.* **2007**, *3*, e117.
[20] a) R. Das, Y. H. Liang, J. Mariano, J. Li, T. Huang, A. King, S. G. Tarasov, A. M. Weissman, X. Ji, R. A. Byrd, *EMBO J.* **2013**, *32*, 2504 – 2516; b) R. Das, J. Mariano, Y. C. Tsai, R. C. Kalathur, Z. Kostova, J. Li, S. G. Tarasov, R. L. McFeeters, A. S. Altieri, X. Ji, R. A. Byrd, A. M. Weissman, *Mol. Cell* **2009**, *34*, 674 – 685.
[21] P. Knipscheer, W. J. van Dijk, J. V. Olsen, M. Mann, T. K. Sixma, *EMBO J.* **2007**, *26*, 2797 – 2807.
[22] D. Reverter, C. D. Lima, *Nature* **2005**, *435*, 687 – 692.
[23] J. Wang, A. M. Taherbhoy, H. W. Hunt, S. N. Seyedin, D. W. Miller, D. J. Miller, D. T. Huang, B. A. Schulman, *Plos One* **2010**, *5*, e15805.

Received: December 7, 2015
Revised: January 29, 2016
Published online: April 1, 2016

